AD-A277 749

CUMENTATION PAGE

| 1. AGENCY USE ONLY (Leave blank)	2. REPORT DATE 1993	3. REPORT TYPE AND DATES COVERED Journal Article

4. TITLE AND SUBTITLE
Evaluation of a hyperbaric system to be used in conjunction with a fluorometer

6. AUTHOR(S)
Colton JS, Grossman Y, Miller K, Pocotte SL

5. FUNDING NUMBERS
PE - 61153
PR - MR04101
TA - 001
WU - 1056

7. PERFORMING ORGANIZATION NAME(S) AND ADDRESS(ES)
Naval Medical Research Institute
Commanding Officer
8901 Wisconsin Avenue
Bethesda, Maryland 20889-5607

8. PERFORMING ORGANIZATION REPORT NUMBER
NMRI 93-103

9. SPONSORING/MONITORING AGENCY NAME(S) AND ADDRESS(ES)
Naval Medical Research and Development Command
National Naval Medical Center
Building 1, Tower 12
8901 Wisconsin Avenue
Bethesda, Maryland 20889-5606

10. SPONSORING/MONITORING AGENCY REPORT NUMBER
DN249512

11. SUPPLEMENTARY NOTES

12a. DISTRIBUTION/AVAILABILITY STATEMENT
Approved for public release; distribution is unlimited.

12b. DISTRIBUTION CODE

13. ABSTRACT (Maximum 200 words)

DTIC
SELECTE
APR 0 4 1994
B

14. SUBJECT TERMS
spectrofluorometer; hyperbaric chamber, high pressure

15. NUMBER OF PAGES
8

16. PRICE CODE

17. SECURITY CLASSIFICATION OF REPORT	18. SECURITY CLASSIFICATION OF THIS PAGE	19. SECURITY CLASSIFICATION OF ABSTRACT	20. LIMITATION OF ABSTRACT
Unclassified	Unclassified	Unclassified	Unlimited

DISCLAIMER NOTICE
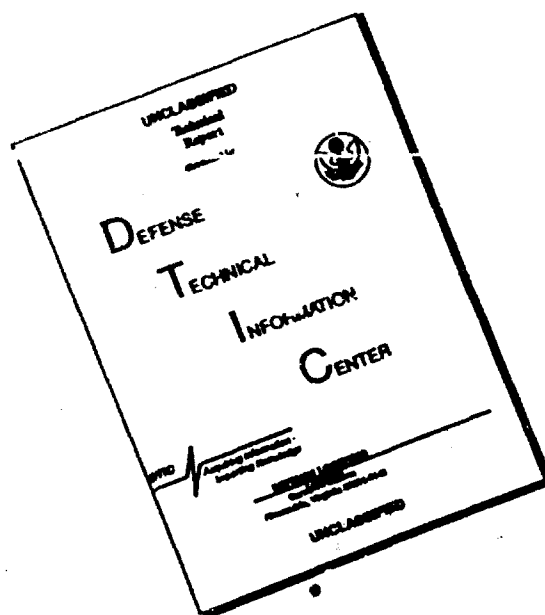
THIS DOCUMENT IS BEST
QUALITY AVAILABLE. THE COPY
FURNISHED TO DTIC CONTAINED
A SIGNIFICANT NUMBER OF
PAGES WHICH DO NOT
REPRODUCE LEGIBLY.

Evaluation of a hyperbaric system to be used in conjunction with a fluorometer

J. S. COLTON, Y. GROSSMAN, K. MILLER, and S. L. POCOTTE

*Dysbaric Diseases and Treatment, Naval Medical Research Institute, Bethesda, Maryland 20889-5055; and
Department of Physiology, Ben-Gurion University of the Negev Beer-Sheva 84105, Israel*

Colton JS, Grossman Y, Miller K, Pocotte SL. Evaluation of a hyperbaric system for use in conjunction with a fluorometer. Undersea & Hyperbaric Med 1993; 20(4):375–382.—A high-pressure chamber that can be used inside the sample chamber of a spectrofluorometer is described and some performance characteristics are presented. The chamber body, constructed of 316 stainless steel, is temperature regulated using resistive heating elements and a microprocessor-based proportional integral derivative controller. The chamber holds a standard 1-cm^2 cuvette that indexes with an electromagnetic stirrer. Injection of different solutions into the closed and pressurized (6.8 MPa) vessel is accomplished by computer-controlled, low-volume solenoids attached to separate microliter injection ports. Repetitive injections of fluids down to a volume of 7 µl are possible in the pressurized chamber. Temperature stability of the chamber is ±0.2°C at atmospheric or elevated pressure. However, during the initial phase (first 3 min) of pressurization, at a compression rate of 0.62 MPa/min, a 0.23°C/min increase in temperature occurs. The chamber windows depress the relative intensity of the emitted light by approximately 20% for visible light and 40% for near UV; however, total sensitivity of the system is sufficient to accomplish most determinations while maintaining a good signal-to-noise ratio. This system can be used to evaluate the response of several molecular and cellular events during compression and at depth with the use of various fluorometric probes.

spectrofluorometer, hyperbaric chamber, high pressure

Through the technique of fluorometry, many chemical, molecular, organelle, or whole-cell events can be monitored in a real-time or near real-time manner with minimal trauma to the preparation (e.g., by impalement with a microelectrode). Thus it is possible to explore the effects of pressure on various aspects of molecular and cellular function in a continuous mode (i.e., before, during, and after pressurization), with the use of fluorometry coupled with an appropriate hyperbaric chamber. Several chambers used in conjunction with fluorometry have been described by other investigators (1–5). There is even a commercially available chamber (SLM Aminco, model HOSC-3K high-pressure spectroscopy cell). Although each of these chambers has unique characteristics, most lack easy sample access and the facility to accurately

and repetitively introduce small quantities of fluids into the sample chamber while fully pressurized.

We describe the physical construction of a high-pressure environmental chamber that is used inside a commercially available fluorometer (Shimatzu, model 540). This chamber can be used to study the effects of custom gas mixtures at ambient or elevated pressures on living tissue. The chamber provides rapid sample access and automated fluid injection. Data are presented to provide a quantitative evaluation of the performance characteristics of the chamber.

METHODS

The hyperbaric chamber was constructed in-house in three sections from 316 stainless steel (Figs. 1 and 2). The overall dimensions of the chamber were 0.5 in. high × 3.62 in. wide × 3.62 in. long for the top and bottom sections and 3.62 in. cubed for the midsection. The midsection contained two 0.62-in. thick × 1-in. diameter fused silica windows (Heraeus Amersil, type T19 Suprasil) set at 90° for passage of the excitation and emission beams (Fig. 2). The windows were secured by inset stainless-steel flanges and flat, rubber gaskets. A 1.5-in. cylindrical bore was machined through the center of the midsection to allow positioning of a plastic cuvette
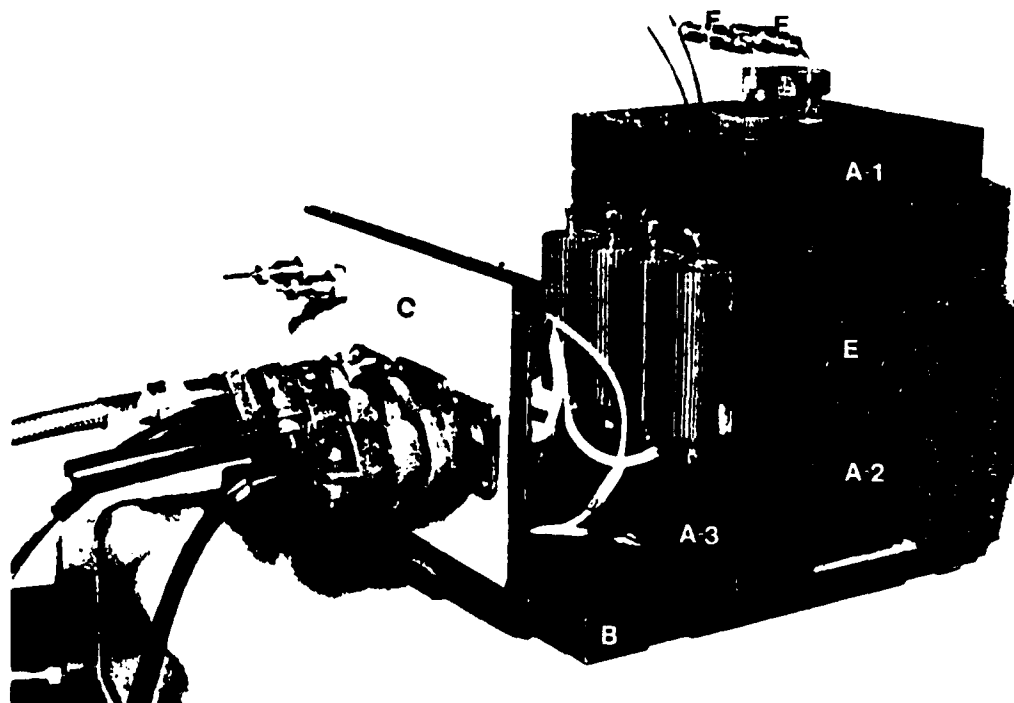

FIG. 1—Photographic view showing: A, three sections of the hyperbaric chamber (top, body, and base); B, the fixed base plate; C, the removable sample compartment wall with feed-through connectors; D, high wattage resistors used for heat exchange; E, fused silica window and retaining flange; and F, zero-volume connectors interfacing PFEK tubing with micro volume stainless steel injection tubes.
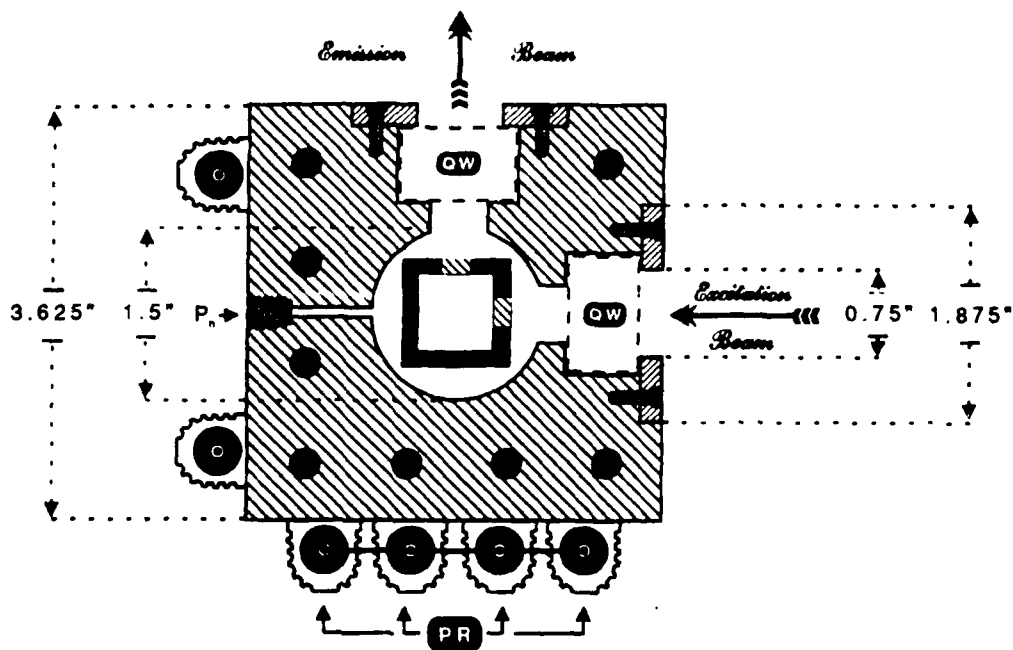
FIG. 2—Cross-sectional view through the center of the steel chamber body. *Center*, central bore containing the fixed cuvette holder; fused silica windows (*QW*); flange securing window to body; penetration port (*Pn*) for RTD or pressurization line; and metal jacketed power resistors (*PR*) for heat exchange.

holder. which was mounted on the bottom section of the chamber. This allowed alignment of the cuvette with the fused silica windows, the excitation beam, and the photodetector. Two small ports were drilled through one side of the chamber wall and opened into the central bore (Fig. 2, *Pn*). These ports were fitted with 0.06-in. male NPT to 0.12-in. Swagelok connectors to provide access for a compression–decompression line and mounting of a stainless-steel-sheathed RTD probe (Omega, model PR-11-2-100-1/8-3-E).

Temperature regulation was achieved by passing current through a group of aluminum-jacketed, 50-W, 2-Ω power resistors (Dale MC 9102) bonded to the chamber with thermal-conductive, electrically insulating epoxy (Tra-Con Inc, Tra-Bond 2151). Temperature control was maintained within 0.1°–0.2°C with a miniature, microprocessor-based proportional integral derivative (PID) temperature controller (Omega, CN 9211A) that was coupled to an 8-A power supply (Arriflex Co, model 339-370). Temperature feedback was provided by the above-mentioned RTD probe.

The contents of the cuvette were continually stirred with a Teflon-coated, slotted, magnetic stirring disk. The stirring disk was propelled by a series of eight epoxy-potted electromagnets located immediately beneath the plastic cuvette holder. A variable rate controller (constructed in-house) was used to synchronize the poles of the eight electromagnets and adjust the stirring frequency.

Injection of microliter quantities of aqueous solutions was made through two feed-through ports in the top of the hyperbaric chamber (Fig. 1*F*). A 3-in. section of 0.06-in. o.d. × 0.01-in. i.d. stainless steel tubing passed through each port and was aligned with the orifice of the quartz cuvette. The external segment of each stainless steel tube was coupled to a 10-in. length of 0.06-in. o.d. × 0.02-in. i.d. flexible PEEK

tubing (Upchurch Scientific Inc, part 1532) via an in-line, zero-volume (0.01 in. i.d)
union (Upchurch Scientific Inc, part U-435). The other end of each PEEK tube was
connected to a separate 0.02-in. i.d. bulkhead union (Upchurch Scientific, Inc, part
U-440) which was mounted through a removable compartment wall of the fluorometer
sample chamber. The flexible, small-bore tubing and zero-volume unions allowed
easy removal and replacement of the chamber lid while maintaining a small "dead
volume."

Control of microliter fluid injection was driven by a dual piston high performance
liquid chromatography minipump (Milton-Roy, model 2396-57) with the output of
each piston directed through a 3.45 MPa, low-volume back-pressure regulator (BPR)
(Upchurch Scientific Inc, part U-463) to separate low-volume, three-way, subminia-
ture, high-speed electronic solenoid valves (General Valve Corp, series 9). With the
solenoid in the "normally open" state, fluid was recirculated through another 3.45
MPa, low-volume BPR (Upchurch Scientific Inc, part U-463) leading to a reservoir
connected to the pump input. Switching the solenoid to the "activated" state, fluid
was selectively directed to the previously described bulkhead union in the removable
compartment wall via 0.06 × 0.02 in. flexible PEEK tubing. The BPRs were used
to preload the pump output and to eliminate retrograde flow during switching at high
pressure, thereby improving the reliability of the delivery of microliter quantities of
fluid to the cuvette in the hyperbaric chamber.

Solenoid switching and timing was regulated via a digital I/O controller (Strawberry
Tree Inc, model ACjr) interfaced with an IBM AT Jr. computer. Position of the
pump pistons was continually sensed with a proximity magnetic reed switch (Alco,
part RS-11-NO) mounted to the pump body and a small magnet permanently attached
to the pump drive shaft. It was possible, therefore, to control fluid ejection through
software manipulations and further increase the accuracy of delivery of microliter
quantities of fluid to the quartz cuvette within the pressurized (6.8 MPa) hyperbaric
chamber. Delivery volumes were determined and calibrated by carefully weighing
ejected aliquots of distilled water and relating the fluid volume to solenoid open time.
To ensure that solenoid activation occurred at the same point of the piston stroke
for each injection, the software design included one or two extra drive-shaft revolu-
tions to compensate for the random signal that initiated the injection cycle.

Bulkhead unions for fluid and gas service to the hyperbaric chamber, as well as
electrical connections for the electromagnetic stirrer and heating resistors, were
located in the removable compartment wall of the fluorometer sample chamber (Fig.
1c). This removable wall was rigidly fixed to a base plate (Fig. 1b) that mounted and
indexed with minimal tolerance to the inside of the fluorometric sample chamber.
The hyperbaric chamber was also rigidly fixed to this base plate. A temporary handle
attached to the top of the hyperbaric chamber allowed convenient removal of the
chamber and its accoutrements as well as easy and precise realignment when the
chamber was reintroduced into the fluorometer sample chamber.

PERFORMANCE CHARACTERISTICS

Temperature control

Initial heating and control parameters for temperature maintenance of the hyper-
baric chamber were determined by the autotune algorithm of the CN9211A tempera-

ture controller. In this manner it was possible to conveniently utilize the three-mode proportional, integrative, and derivative (PID) control function.

The time to heat the chamber mass was approximately 30 min, with thermal stability occurring at about 80 min after the initial "power-up." Temperature variation of the chamber mass did not exceed ±0.2°C after the initial 80-min warm-up period. The same degree of temperature stability was observed for the chamber mass during linear He–O$_2$ pressurization to 6.8 MPa at dive rates of 0.62, 0.94, or 124 MPa/min.

Even though the temperature of the chamber mass remained relatively constant during rapid pressurization, the temperature of the chamber cavity varied with pressure, thus causing the temperature in a fluid-filled cuvette (3 ml normal saline) to fluctuate in a similar manner. At a dive rate of 0.62 MPa/min the maximal rate of heating occurred during the first 1.17 MPa (3 min) of the dive 0.23°C/min) (Fig. 3). Temperature stabilized during the remainder of the dive, varying no more than ±0.2°C. After reaching 6.8 MPa the fluid in the cuvette began to cool, stabilizing after 10 min at pressure (Fig. 3).

Optics

The path length or thickness of each fused silica window used in the hyperbaric chamber influenced the optical transmission; therefore, selection of the appropriate thickness for a given diameter window to function safely at elevated pressure was critical. Optimal window thickness was determined from a nomograph supplied by the manufacturer (Heraeus Amersil), relating window diameter and working pressure. With a working pressure of 6.8 MPa (safety factor = 10×) and window diameter of 1 in., minimal thickness was determined to be 0.60 in.

From product specifications supplied by the manufacturer, a theoretical loss of transmitted light through the two windows of approximately 16–20% was calculated for light radiation between 250–700 nm. These losses were a function of reflective losses at the outside surfaces, the path length, the coefficient of absorption for the particular glass, and the refractive index of the glass. The actual influence of the
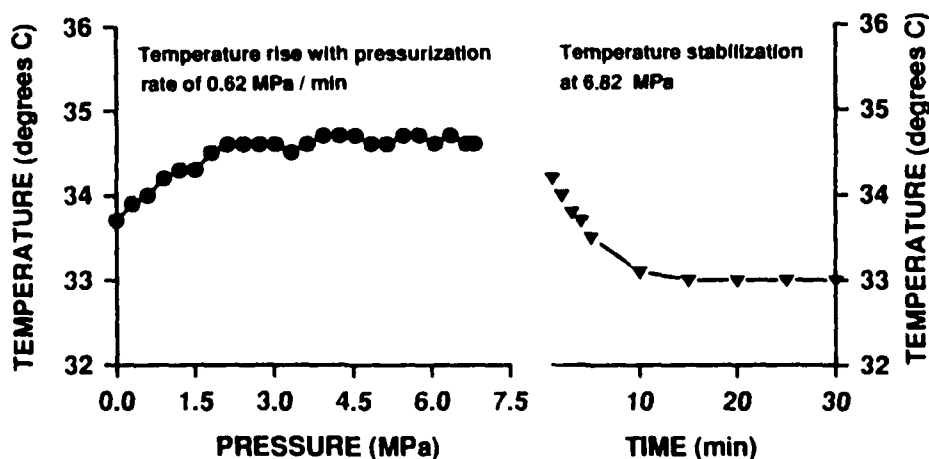

FIG. 3—Effect of compression on temperature of a fluid-filled cuvette (3 ml) inside the closed chamber. *Left*, typical temperature changes occurring with compression; *right*, temperature response immediately after compression has been halted at 6.82 mPa and further monitored for 30 min at this pressure.

two fused silica windows in the hyperbaric chamber on transmitted light was determined by measuring the relative fluorescence of a particular fluorophore in the standard fluorometer sample compartment and repeated in the hyperbaric chamber, which was positioned inside the sample compartment of the fluorometer. The actual decrease in fluorescence intensity was within the predicted range for three of the four dyes tested; for fluorescein, 9-aminoacridine, 3,3'-diethylthiadicarbocyanine iodide, and norepinephrine. fluorescence decreased 22.6, 15.8, 18.3, and 40.7%, respectively (Table 1). The most profound loss (40.7% for norepinephrine) occurred in the area of near UV band (280 nm excitation and 314 nm emission).

Fluid injection

To enhance the utility of the chamber, microliter fluid injection into the quartz cuvette was accomplished by computer-controlled solenoid switching and a high-pressure minipump. The smallest volume that could be consistently delivered in a repetitive manner was determined by a combination of the flow developed by the pump and the solenoid switching rate. For the model pump used in this system, maximum flow was 80 μl per stroke, delivered in less than 70 ms. Solenoid response time was less than 6 ms. With stroke volume set to 100% it was possible to repetitively inject 7–75 ± 3 μl at both atmospheric and high pressure. Calibration curves (not shown) demonstrated a linear relation between solenoid "open time" and "volume delivered" over the single-stroke injection range. It was necessary, however, to construct separate calibration curves at atmospheric and hyperbaric pressure for each solenoid.

DISCUSSION

The chamber described in this paper has the capability to allow continuous monitoring of fluorescent or chemiluminescent events in molecular, organelle, or cell suspensions, as well as cells adhered to glass coverslips, while in a normobaric atmosphere, during compression, or at high pressure. The performance tests have shown that the system controls chamber and cuvette temperature to within 0.2°C during steady-state conditions. During compression, control of the chamber temperature continues to hold within 0.2°C, but cuvette temperature can warm as much as 1°C depending

Table 1: Influence of Silica Windows on the Relative Intensity of Excited Dyes

| Dye | λ_{EC} | λ_{EM} | Relative Intensity | | |
			W/O HC	HC	Decrease, %
3,3'-Diethylthiadicarbocyanine	650	668	71.0	58.0	18.3
9-Aminoacridine	400	455	84.7	71.3	15.8
Fluorescein	357	533	94.0	72.8	22.6
Norepinephrine	280	314	80.0	47.4	40.7

Key: λ_{EC} = excitation wavelength (nm); λ_{EM} = emission wavelength (nm); W/O HC = relative intensity of dye determined in the sample compartment without hyperbaric chamber; HC = relative intensity of dye determined with hyperbaric chamber in sample compartment.

on compression rate. Microliter fluid injection can be accomplished at either atmospheric or hyperbaric pressures with a minimal, repetitive volume of 7 μl. Continual stirring within the cuvette prevents suspensions from settling and promotes rapid mixing of injected substances.

A large number of fluorescent and chemiluminescent probes have become commercially available (Molecular Probes, Inc.; Eastman Kodak Co.) for the investigation of various molecular and cellular processes. The incorporation of fluorescent techniques in a hyperbaric environment could provide a powerful tool with which to study many of the phenomena associated with high-pressure alteration of physiologic and biochemical function. Several investigations have demonstrated this capability (1–5). Of particular interest to this laboratory is the effect of high pressure on neuronal function. For example, several investigations have demonstrated a pressure-dependent depression of neurotransmitter release which may be attributable to changes in transterminal calcium flux (8–11) or altered vesicle fusion (12). It is also possible that other molecular mechanisms of neurotransmitter release are influenced by pressure; for example, alteration in calcium–calmodulin interaction, interference with various "docking" proteins, or disruption of transmembrane potential or surface charges. Utilizing a range of different fluoroprobes and chemiluminescent indicators in a hyperbaric environment, in association with different model systems such as cultured neurons, synaptosomes (8, 9), PC12 cells (13), or isolated molecules such as calmodulin (14), glutamate (15, 16), or glutamate decarboxylate (17), it is possible to evaluate these "models" in a rapid, real-time, continuous mode. From information provided by the various techniques and a hierarchy of model systems, it is anticipated that the mechanism(s) of action of gases at high pressure on intact brain will be more fully understood.

REFERENCES

1. Chong PL-G, Fortes PAG, Jameson DM. Mechanisms of inhibition of (Na,K)-ATPase by hydrostatic pressure studied with fluorescent probes. J Biol Chem. 1985; 260:14484–14490.
2. Chryssomallis GS, Drickamer HG, Weber G. The measurement of fluorescence polarization at high pressure. J Appl Physiol 1978; 49:3084–3087.
3. Jona I, Martonsi A. The effect of high pressure on the conformation, interactions and activity of the Ca2+-ATPase of sarcoplasmic reticulum. Biochim Biophys Acta 1991; 1070:355–373.
4. Paladini AA, Weber G. Absolute measurements of fluorescence polarization at high pressures. Rev Sci Instrum 1981; 52:419–427.
5. Philp RB, Arora P, McIver DJ. Effects of gaseous anesthetics and ultrashort and short-acting barbiturates on human blood platelet free cytosolic calcium: relevance to their effects on platelet aggregation. Can J Physiol Pharmacol 1992; 70:1161–1166.
6. Mayevsky A. Brain NADH redox state monitored in vivo by fiber optic surface fluorometry. Brain Res 1984; 319:49–68.
7. Mayevsky A, Shaya B. Factors affecting the development of hyperbaric oxygen toxicity in the awake rat brain. J Appl Physiol 1980; 49:700–707.

8. Gilman SC. Colton JS. Dutka AJ. Boogaard J. Effects of high pressure on the release of excitatory amino acids by brain synaptosomes. Undersea Biomed Res 1986; 13:397–406.
9. Gilman SC. Colton JS. Grossman Y. A23187 stimulated calcium uptake and GABA release by cerebrocortical synaptosomes: effects of high pressure. J Neural Transm 1991; 86:1–9.
10. Grossman Y. Colton JS. Gilman S. Interaction of Ca-channel blockers and high pressure at the crustacean neuromuscular junction. Neurosci Lett 1991; 125:53–56.
11. Grossman Y. Kendig JJ. Evidence for reduced presynaptic Ca + 2 entry in a lobster neuromuscular junction at high pressure. J Physiol (Lond) 1990; 420:355–364.
12. Heinemann SH. Conti F. Stuhmer W. Neher E. Effects of hydrostatic pressure on membrane processes: sodium channels. calcium channels and exocytosis. J Gen Physiol 1987; 90:765–778.
13. Greene LA. Rein G. Release. storage and uptake of catecholamines by a clonal cell line of nerve growth factor (NGF) responsive pheochromocytoma cells. Brain Res 1977; 129:247–263.
14. Johnson DJ. Wittenauer LA. A fluorescent callmodulin that reports the binding of hydrophobic inhibitory ligands. Biochem J 1983; 211:473–479.
15. Nicholls DG. Sihra TS. Sanchez-Prieto J. Calcium-dependent and independent release of glutamate from synaptosomes monitored by continuous fluorometry. J Neurochem 1987; 49.50–57.
16. Graham LT. Aprison MH. Fluorometric determination of aspartate. glutamate. and γ-aminobutyrate in nerve tissue using enzymic methods. Anal Biochem 1966; 15:487–497.
17. Colton JS. Gilman S. Chang P. Colton CA. Effect of helium and heliox on glutamate decarboxylase activity. Undersea Biomed Res 1990. 17:297–303.